

Review Article

An Overview on the Photocatalytic Activity of Nano-Doped-TiO₂ in the Degradation of Organic Pollutants

Yong Nian Tan, Chung Leng Wong, and Abdul Rahman Mohamed

School of Chemical Engineering, Universiti Sains Malaysia, Engineering Campus, Seri Ampangan, Seberang Perai Selatan, Pulau Pinang, 14300 Nibong Tebal, Malaysia

Correspondence should be addressed to Abdul Rahman Mohamed, chrahman@eng.usm.my

Received 11 September 2011; Accepted 19 October 2011

Academic Editors: D. Chicot and P. Sánchez

Copyright © 2011 Yong Nian Tan et al. This is an open access article distributed under the Creative Commons Attribution License, which permits unrestricted use, distribution, and reproduction in any medium, provided the original work is properly cited.

This paper aims to review and summarize the recent works on the photocatalytic degradation of various organic pollutants in the presence of nano-doped-TiO₂ photocatalysts. In this regard, three main aspects are examined: (a) the presence of various dopants (metal dopants, nonmetal dopants, halogen dopants, metalloid dopants, and codopants) in the formation of nano-doped-TiO₂ photocatalysts, (b) the effect of the presence of dopants on the photocatalytic degradation of organic pollutants, and (c) the effects of various operating parameters on the photocatalytic degradation of organic pollutants in the presence of nano-doped-TiO₂ photocatalysts. Reports resulted suggest that the formation of a high percentage of the anatase phase, small crystallite size, and high specific surface area of the nano-doped-TiO₂ photocatalysts depends on the presence of various dopants in the photocatalysts. The majority of the dopants have the potential to improve the photocatalytic efficiency of nano-doped-TiO₂ in the degradation of organic pollutants. The photocatalytic degradation of organic compounds depends on the calcination temperature of the prepared doped TiO₂, initial reactant concentration, dosage of doped TiO₂, and dopant doping concentration.

1. Introduction

Water reuse has emerged as a critical issue in preserving global water resources in recent times. In many developing countries, industries contribute around 22% of the total world water usage and around 70% of untreated industrial wastes are simply discarded into wastewater without prior filtering or processing. The world faces enormous challenges ahead as drinkable water runs short due to natural disasters, population increase, and water pollution. To address these problems, advanced oxidation processes (AOPs) play an important role in the wastewater treatment. In AOPs, highly reactive radicals are generated that can treat the toxic and nondegradable pollutants in the wastewater efficiently without involving complex technologies [1].

The nano-TiO₂ photocatalyst is a well-known photocatalyst among the metal oxides recognized for its high efficiency, low cost, physical and chemical stability, widespread availability, and noncorrosive property [2]. When nano-TiO₂ is irradiated with ultraviolet (UV) light, electron is promoted from the valence band to the conduction band, resulting in

the generation of energized “holes” in the former. Free electrons react with the oxygen to form superoxide radical anions (O₂^{•-}), while energized holes react with water (H₂O) or hydroxyl ion (OH⁻) to form hydroxyl radicals (•OH). However, these reactive species are lost when the excited electrons and energized holes recombine without invoking a photocatalytic effect. Such electron-hole recombination diminishes the efficiency of photocatalysis.

To achieve high photocatalytic degradation efficiency, nano-TiO₂ should be mesoporous and should exhibit high crystallinity and high specific area [3]. Nano-TiO₂ is normally synthesized using various titania precursors such as titanium tetra-iso-propoxide (TTIP) [4], tetrabutyl titanate (TBOT) [5], titanium tetrachloride (TiCl₄) [6] besides other titanium compounds. Different starting materials can influence the morphology of the nano-TiO₂ produced. For example, Verma et al. [7] reported that various types of alkoxy group in titanium alkoxide (Ti(OPr)₄ and Ti(OPrⁱ)₄) showed different properties of the mixed CeO₂-TiO₂ films. Zhang et al. [8] also stated that different types of starting

materials of nano-TiO₂ (titanium alkoxides and inorganic titanium, which are titanium sulfate and titanium chloride) could affect the properties of TiO₂/adsorbent nanostructured composites (TNC). Zhang et al. [8] found that chloride (Cl⁻) ions could promote the aggregation of titanium oxide species on the surface of activated carbon and the formation of the rutile TiO₂ phase. On the other hand, the presence of sulfate (SO₄²⁻) ions could enhance the photocatalytic activity of nano-TiO₂ [8]. At present, the effects of starting materials on the formation of nano-TiO₂ have not been fully explored despite efforts that have been made to this end. Even though a complete understanding has yet to be achieved, it is generally accepted that titanium dioxide precursors affect the morphology of nano-TiO₂ in aspects such as specific surface area, crystallinity phase, and crystallite size that play an important role in the photocatalytic degradation of organic pollutants [9].

It is clear from the literature that small crystallite size, high percentage of the anatase phase, and high specific surface area of nano-doped-TiO₂ increase the photocatalytic degradation efficiency. For example, Venkatachalam et al. [10] found that the addition of magnesium nitrate during the formation of nano-doped-TiO₂ by the sol-gel method promoted the exclusive formation of the anatase phase. The consequent enhanced adsorption of 4-chlorophenol over nano-doped-TiO₂ and the decrease in particle size of nano-doped-TiO₂ increased photocatalytic degradation of 4-chlorophenol [10].

Doping techniques have been applied in photocatalysis to overcome the limitations of nano-TiO₂, such as a wide band gap, ineffectiveness of photocatalysis under sunlight, and thermal instability [8, 11]. Basically, nano-TiO₂ can only utilize 6% of the total solar irradiation in photocatalysis due to the large band gap of anatase nano-TiO₂ (3.2 eV), but doping techniques shift the activity of nano-doped-TiO₂ from the UV region to the visible light region [12]. This paper appraises different doping techniques [13] that widen the photocatalytic range from the ultraviolet to the visible light region, thus allowing for the photocatalytic degradation of organic pollutants under solar irradiation [14–17].

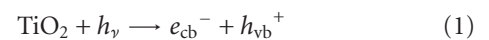
There are also negative effects of doping techniques in the photocatalytic performance of nano-doped-TiO₂. Firstly, the dopant can act as a charge recombination center that acts against the separation of excited electron and hole. Secondly, doping techniques can inhibit the production of oxygen radicals in the photocatalysis reaction [18]. However, these problems can be countered by controlling the dosages of the dopants. Besides shifting the wavelength sensitivity of nano-doped-TiO₂ into the visible light range, doping techniques can also improve the physical properties of TiO₂. Cai et al. [19, 20] reported that suitable amounts of dopants helped to control the crystallite size of nano-doped-TiO₂ while producing a high specific surface area of nano-doped-TiO₂. A judicious rate of doping also prevented the transformation of the anatase phase to the rutile phase.

In this paper, studies on the modification of nano-TiO₂ photocatalysts with various types of dopants are reviewed.

The photocatalytic activity of TiO₂ incorporating various dopants doping processes on the photocatalytic degradation of organic pollutants are assessed. The effects of various operating parameters on the photocatalytic degradation of organic pollutants in the presence of nano-doped-TiO₂ photocatalysts are also appraised.

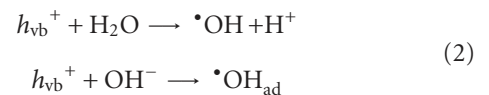
2. Short Background Regarding Photocatalytic Degradation Process

According to Pirkanniemi and Sillanpää [21], the overall heterogeneous photocatalysis can be summarized into the following five steps: (1) reactant diffusion to catalyst surface, (2) adsorption of reactant onto the surface, (3) chemical reaction on the catalyst surface, (4) desorption of final products off the catalyst surface, and (5) diffusion of final products from the catalyst surface. Heterogeneous photocatalysis is a favorable combination of charge transport features, electronic structures, excited-state life spans, and light absorption effects. The basis of photocatalysis is the photo-excitation of a semiconductor that is solid as a result of the absorption of electromagnetic radiation, often, but not exclusively, in the near UV spectrum. When the energy (photon) supplied is equal to or greater than the band gap energy, ΔE_g of the photocatalyst, the excited electron in the valence band is transferred to the empty conduction band. (The band gap energy is the difference in energy between the valence band and conduction band of the photocatalyst. It is in the order of a few electron volts.) This leads to the generation of a positive hole (h_{vb}^+) in the valence band and an electron (e_{cb}^-) in the conduction band. As a result, electron-hole pairs are generated in the photocatalytic reaction



where h_ν is energy required to transfer the excited electron from the valence band to the empty conduction band.

In this reaction, the positive hole and electron are powerful oxidizing and reducing agents, respectively. Generally, the positive hole reacts with either surface-bound water (H₂O) or pollutant to produce hydroxyl radical ($\cdot\text{OH}$) and surface adsorbed hydroxyl radical ($\cdot\text{OH}_{ad}$).

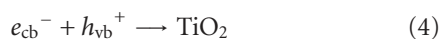


On the other hand, the electron in the conduction band is picked up by an electron acceptor such as oxygen to produce superoxide radical anion (O₂^{•-}).



Basically, the oxidative and reductive reactions do not occur concurrently. Hence, when an accretion of electron occurs in the conduction band, the electron is then recombined with the positive hole in the absence of the photocatalyst. As the photocatalytic reaction proceeds in preference to the positive hole-electron recombining, efficient electron

consumption is hence essential to promote the photocatalytic oxidation. The equation of the recombination of positive hole and electron is shown below:



Thus, the organic pollutant is oxidized to form salts, carbon dioxide, and water in the complete photocatalytic oxidation process.



3. Effects of Dopants in the Formation of Nano-Doped-TiO₂

Titanium dioxide is a well-known photocatalyst that is not only sensitive to light and corrosion resistant, but also inexpensive as an industrial material [22]. However, there are disadvantages linked to the use of TiO₂ as a photocatalyst. These include the difficulty in producing high-grade TiO₂ with tightly controlled physical properties and the fact that, in its basic form, it functions only under UV irradiation [23]. Many factors govern the physicochemical properties of TiO₂ during its production such as the speed of growth, the diffusion coefficient, and the ionic radii [24]. The method of preparation and posttreatment conditions also play prominent roles in synthesizing a high efficiency TiO₂ product [25]. To overcome some of the difficulties encountered, different dopants (metal and non metal) are being investigated with the aim of enhancing the morphology of TiO₂ in the photocatalysis [26].

Dopants modify the electronic structure of nano-TiO₂ to broaden its effective range of light sensitivity for photocatalysis from the ultra-violet (UV) region to the visible light region [27]. Doping techniques have been shown to be effective and efficient despite their being susceptible to thermal instability and their requirement for expensive ion-implantation facilities [28]. Dopants are valued for their ability to confer excellent physicochemical properties such as high crystallinity (high percentage of anatase phase), high specific surface area, and small crystallite size [20, 29]. There are three types of crystalline phases of nano-TiO₂, namely, the rutile, anatase, and brookite phases. The anatase and rutile phases are the common crystallographic phases found in the formation of nano-TiO₂, with the former particularly favored for its high photocatalytic activity [30] and exceptional thermodynamic stability in nanoscale dimensions [9]. The crystalline structure of nano-TiO₂ is represented as a TiO₆ octahedral. The formation of the anatase and rutile phases or phase transformation from anatase to rutile is strongly dependent on the thermal dehydration process during which time; Ti–O–Ti bonds are formed by the interaction between –OH groups and the protonated surfaces.

Specific surface area of TiO₂ is one of the factors that determine the morphology of TiO₂ in photocatalysis. A large specific surface area of TiO₂ enhances the photocatalytic degradation rate of organic pollutants as availability of active sites in TiO₂ is increased [31, 32]. Crystallite size

is another important characteristic that determines the quality of TiO₂. The performance of nano-TiO₂ can be enhanced in the photocatalysis by producing nano-doped-TiO₂ with high crystallite size up to a certain limit [33]. Thereafter, the photocatalytic performance of nano-doped-TiO₂ decreases when the crystallite size falls beyond this limit because of the trapping of charge carriers during the diffusion process. With the presence of dopants in the formation of nano-doped-TiO₂, the phase transformation from anatase to rutile inhibits when the thermal energy is low enough to overcome the nucleation barrier during the thermal dehydration process, and this occurs more readily with the smaller crystallite size of nano-doped-TiO₂ [34]. In short, dopants suppress the crystallite size of nano-TiO₂ by inserting itself into the lattice structure of the nano-doped-TiO₂ octahedral to modify its physicochemical properties. In general, a smaller crystallite size of nano-doped-TiO₂ is favored compared to larger crystallite size of nano-doped-TiO₂ since the smaller size reduces the recombination of the photogenerated charge carriers [35]. Some researchers reported that smaller crystallite size of nano-doped-TiO₂ induced a larger band gap due to the increased redox ability [31]. The resultant photocatalytic activity benefits from the quantum size effect of nano-doped-TiO₂ that enhances its photocatalytic activity [32].

In another studies, some researchers found that the presence of dopants did not affect the morphology of nano-doped-TiO₂ [36, 37]. For example, Nahar et al. [36] noted that Fe dopant, even at high concentrations, did not change the crystalline phase of nano-doped-TiO₂. Li et al. [37] stated that cerium ions had no obvious effect on the particle size, morphology, and crystalline phase of nano-doped-TiO₂.

Although nano-TiO₂ with large specific surface area, high percentage of anatase phase, and small crystallite size all contribute towards high photocatalytic activity, a complete understanding of the interlinkages between these variables has yet to be achieved and their detailed underlying mechanisms remain a challenge to researchers.

3.1. Effect of Metal Doping. Metal dopants have been used to improve the morphology and photocatalytic activity of nano-doped-TiO₂. In previous studies, various metal dopants, including cobalt (Co) [38, 39], barium (Ba) [40], manganese (Mn) [41], nickel (Ni) [42], copper (Cu) [43], zinc (Zn) [44], and iron (Fe) [45, 46], have been analyzed for their abilities to enhance the photocatalytic performance of nano-doped-TiO₂. They improve nano-doped-TiO₂ performance under visible light irradiation by shifting the absorption spectra to a lower energy region [47]. In addition, various approaches have been attempted to sustain photocatalytic activity by limiting the recombination of the photogenerated electron-hole pairs in photocatalysis.

Hsieh et al. [38] produced codoped titania nanotubes with a specific surface area of 379 m²/g, outer diameter of 10–15 nm, and inner diameter of 5–10 nm. Suriye et al. [39] found that codoped TiO₂ exhibited high anatase phase based on X-ray diffraction (XRD) patterns. Smaller particle size of Ba-doped TiO₂ were synthesized by Atashfaraz et al. [40] who reacted titanium dioxide and barium hydroxide

at high temperature in the flow reactor. Zhang et al. [41] produced Mn-doped TiO₂ using the sol gel method. Based on their observations, the band gap of the photocatalyst was narrowed due to the formation of an impurity level near the bottom of the conduction bands. Xu et al. [44] showed that Zn which was located on the titania nanotube surface had little effect on the titania nanotube morphology. Fe-doped titania prepared by Janes et al. [45] using the sol gel method prevented the phase transformation of anatase to rutile at low dopant levels. The interaction was applicable to a maximum Fe dopant loading of 5.64 wt%. Deng et al. [46] also investigated the morphology of Fe-doped titania nanotubes synthesized by the sol gel and hydrothermal methods. They found that the addition of Fe slowed the crystallization process and prevented the growth of crystallite TiO₂.

Besides metal dopants, transition metals dopants such as palladium (Pd), chromium (Cr), and silver (Ag) have been investigated by Wu et al. [48] to enhance the photocatalytic performance of nano-doped-TiO₂. Among the transition metals dopants tested, Pd ion had the strongest interaction with nano-TiO₂ and improved its morphology most effectively. Some researchers are of the opinion that doping techniques promote the production of smaller crystallite nano-doped-TiO₂ with the resultant larger surface area helping to prevent the problem of particle agglomeration [49].

Among the metal dopants, Fe³⁺ ions reportedly benefit from uniform distribution into the lattice structure of TiO₂ because of the similarity of their ionic radii [50]. Fe³⁺ ions are also thought to control the crystallite size of TiO₂ and prevent the phase transformation of the anatase phase to the rutile phase. Deformation of the TiO₂ crystal lattice occurs when Fe³⁺ ions (0.690 Å) merge with Ti⁴⁺ ions (0.745 Å), restricting the growth of Fe-TiO₂ crystallite size in the process.

Fe³⁺ ions have also been reported to act as shallow charge traps in the lattice of TiO₂, and this accounts for its high photocatalytic activity [51]. This is explained by the conduction band edge of TiO₂ being above the energy level for Fe³⁺/Fe²⁺, whereas the valence band edge of TiO₂ is below the energy level for Fe³⁺/Fe⁴⁺ [49]. Hence, Fe³⁺ can react easily with the photogenerated electron (from conduction band of TiO₂) and the hole (from valence band of TiO₂) to form Fe²⁺ and Fe⁴⁺ ions. In this manner, Fe³⁺ ions can enhance the lifetime of the electrons and holes by acting as both electron and hole traps (Fe²⁺ and Fe⁴⁺ ions). Nevertheless, Fe²⁺ and Fe⁴⁺ ions are not stable compared with Fe³⁺ ions due to the half-filled 3d⁵ orbital.

The choice of different starting Fe materials affects the morphology of TiO₂ that is produced. For instance, FeCl₃ is widely used as a dopant because its Cl⁻ ions are weakly bonded to the TiO₂ surface as compared with Fe³⁺ ions. This facilitates the incorporation of Fe³⁺ ions, in preference over Cl⁻ ions, onto the TiO₂ surface. Consequently, Fe-doped TiO₂ with Brunauer-Emmett-Teller (BET) surface area of 100 m²/g, crystallite size of <9 nm, and the presence of anatase phase can be obtained by adding less than 1 wt% Fe [49, 50, 52–54].

Some of the researchers found that judicious doping with Fe improves TiO₂ morphology, but specific surface area suffers beyond the optimum doping level [50, 52]. This is because Fe acts as a recombination center for both free electrons and energized holes [53, 54], thus limiting the interaction between Fe and TiO₂ [49]. In addition, Fe induces the formation of amorphous titanium(IV)-iron(III)-oxide that leads to the inhibition of the anatase phase of TiO₂ [55]. The optimum Fe loading (0.007–1.200 wt%) gives a combination of crystallite size (9.0–23.7 nm) and specific surface area (55.5–175.0 m²/g) of TiO₂ [49, 50, 53–56].

The foregoing notwithstanding, there are other researchers who are of the view that the Fe is not requisite for the improvement of TiO₂ characteristics. Li et al. [51] produced Fe-doped TiO₂ with particle size of 10–15 nm via the hydrothermal method. They also reported that increasing the amount of Fe could narrow the band gap of TiO₂ by shifting its activity from UV region to the visible light region. Based on an observation from X-ray photoelectron spectroscopy (XPS), Fe was thought not to be located on the TiO₂ surface, but was positioned within the matrix interior. Thus, the isolated Fe³⁺ had a lower chance of transferring the trapped charge carriers to the interface and this could account for a decrease in photocatalytic activity, for example, in the degradation of methylene blue.

Sakthivel et al. [57] investigated the performance of TiO₂ after supplementing with platinum (Pt) dopant. Pt acted as an electron trap in the formation of TiO₂, decreasing its surface area. While the generated free electrons gravitated towards Pt that served as a temporary electron trap preventing electron-energized hole recombination, increased Pt also competed with TiO₂ as an electron trap to decrease effective surface area in the latter. A further increase in Pt dopant might lead to the following possible consequences: (1) shortening of the charge carrier space distance [57], (2) recombination of free electron and energized hole [58], (3) agglomeration of Pt and TiO₂ [58], and (4) decrease in the probability of oxygen being photo-adsorbed on TiO₂ [57]. The crystallite size of 9.15–31.00 nm and a specific surface area of 19.1–118.7 m²/g of TiO₂ was produced by loading Pt at the rate of 0.1–1.5 wt% [56, 58–61].

Chromium (Cr), cerium (Ce), and vanadium (V) have also been used as dopants for TiO₂. The addition of vanadium (V) increases the surface area and porosity of TiO₂ [62]. The advantages of Ce as dopants include (1) decrease of the rate of crystallite growth, (2) promotion of mesoporous materials formation, (3) promotion of the stability of the active phase, (4) prevention of thermal loss in the catalyst area [63], and (5) prevention of the phase transformation of the anatase to the rutile phase [63].

Metal-doped TiO₂ products reveal the presence of the anatase phase and a crystallite size of TiO₂ ranging from 2.59 to 12.00 nm. The specific surface area of TiO₂ is in the region of 100–500 m²/g [49, 50, 52–60, 62–66]. Table 1 which summarizes the dopants used in TiO₂ formation shows that different dopants are responsible for different structural properties of the TiO₂. Further studies are needed to understand the mechanism of metal doping in the

TABLE 1: Properties of metal-doped TiO₂ photocatalysts under various conditions.

Type of metal dopant	(Metal dopant/TiO ₂) molar ratio	Preparation of doped TiO ₂	Starting material of TiO ₂	Starting material of metal dopants	Crystallite size (nm)	Phase	BET surface area (m ² /g)	Reference
Fe	0.090	Hydrothermal	TTB	FeCl ₃ , FeCl ₂	11.40	Anatase	101.40	[50]
	0.100	Hydrothermal	(Ti(OC ₄ H _{9-n}) ₄) ₄	Fe(NO ₃) ₃ •9H ₂ O	14.50	Anatase	102.00	[53]
	1.200	Hydrothermal	TiCl ₃	FeCl ₃ •6H ₂ O	23.70	Anatase	55.50	[55]
	0.007	Sol gel	TTIP	Fe(NO ₃) ₃	—	Anatase	175.00	[54]
	0.700	Sol gel/microemulsion	TTIP	Fe(NO ₃) ₃	12.70	Anatase	83.00	[52]
	0.980	Sol gel	Ti(OPr ⁱ) ₄	Fe(NO ₃) ₃ •9H ₂ O	9.00	Anatase	126.10	[49]
Pt	0.800	Impregnation	TiO ₂ Degussa P25	PtCl ₂	22.28	Anatase	29.17	[57]
	1.000	Impregnation/Photodeposition	TiO ₂ Degussa P25	H ₂ PtCl ₆	20.00	Anatase	107.00	[64]
	1.500	Impregnation	TTIP	H ₂ PtCl ₆	31.00	Anatase	19.10	[61]
	0.500	Photochemical deposition	TBOT	H ₂ PtCl ₆ •6H ₂ O	9.15	Anatase	116.10	[60]
	1.500	Photochemical reduction	TNBT	H ₂ PtCl ₆ •6H ₂ O	—	Anatase	118.70	[58]
Ce	0.100	Sol gel	TiCl ₄	H ₂ PtCl ₆ •6H ₂ O	14.00	Anatase	68.00	[59]
	0.010	Hydrothermal	Ti(SO ₄) ₂	Ce(NO ₃) ₄	—	Anatase	454.00	[63]
	4.000	Reflux	Ti(OBu) ₄	Ce(NO ₃) ₄	8.30	Anatase	—	[65]
V	1.000	Sol gel	Ti(OBu) ₄	VO(OPr) ₃	12.00	Anatase	107.00	[62]

formation of TiO₂ and the influence of metal dopants in its morphology.

3.2. Effect of Nonmetal Doping. Various approaches have been made in the bid to hinder recombination of the photo-generated electron-hole pairs in nano-TiO₂. Nonmetal anion doping has been exhaustively investigated because the electronic states of nonmetals are above the valence band edge of TiO₂ compared with pure TiO₂. Accordingly, different nonmetal dopants including carbon (C), nitrogen (N), and sulfur (S) have been tested for their ability to improve the morphology and photocatalytic performance of TiO₂ [73, 74]. The presence of nonmetal anions increases the percentage of the anatase phase in TiO₂, restrains the growth of crystallite size of TiO₂, and increases the specific surface area of TiO₂ [75]. Besides, doping with nonmetal anions broadens the band gap of TiO₂ in its electronic structure and affects the red-shift in the absorption spectra of nano-doped-TiO₂. In this way, various photocatalytic, photochemical, and the photoelectrochemical properties of TiO₂ are enhanced by shifting the wavelength sensitivity of TiO₂ from ultra violet region into the visible light region [73]. A summary of properties of various nonmetal dopants of TiO₂ under various conditions is given in Table 2.

Phosphorus (P) is used as a nonmetal dopant to enhance the thermal stability of TiO₂ through the formation of titanyl phosphate [68]. In addition, P also improves the surface properties of TiO₂ and reduces the oxygen vacancies, thus improving the performance of TiO₂ in other applications such as photocatalysis and gas sensing [67]. High specific surface area of 154 m²/g and crystallite size of 8.6 nm of nano-doped-TiO₂ have been successfully produced at a P/Ti

molar ratio of 0.14 [68]. Phosphorus doped TiO₂ displays a larger specific surface area and smaller crystallite size as compared with pure titania [67].

Nitrogen (N) has been reported to generate better dispersion, uniform particle size distribution, and uniform surface area when used to dope TiO₂ in the hydrothermal process [76]. Senthilnathan and Phillip [70] obtained 22 nm of crystalline size of N-doped TiO₂. Nitrogen atoms substitute for the oxygen atoms in TiO₂ lattice to form O-Ti-N. This substitution phenomenon is consistent with the findings of Peng et al. [69] who established 21% as the highest acceptable nitrogen dopant concentration in N-TiO₂.

Doping sulfur atoms into the TiO₂ lattice improves the photocatalytic efficiency under visible light irradiation [72]. When fine crystalline S-doped TiO₂ was synthesized in the study of Ho et al. [72] through a simple hydrothermal method, the optical absorption of S-doped TiO₂ in the visible light region increased in tandem with the increase in the S content. This may be related to the finding by Tian et al. [71] that the anatase/rutile phase composition ratio was strongly influenced by the amount of S. The phase composition ratio increased with the increase in S amount, with TiO₂ doped with 1.5% S displaying the best crystallite size (around 30 nm).

3.3. Effect of Metalloid and Halogen Doping. Halogen doping techniques have been made in the bid to hinder the transformation of anatase to rutile phase in nano-doped-TiO₂ photocatalysts. The developments of halogen-doped TiO₂ photocatalysts have attracted high attentions due to their ability in substituting into TiO₂ matrix. Meanwhile, halogen doping could improve the surface properties as well as

TABLE 2: Properties of non metal-doped TiO₂ photocatalysts under various conditions.

Type of non-metal dopant	(Non metal dopant/TiO ₂) molar ratio	Doped TiO ₂ preparation method	Starting material of TiO ₂	Starting material of non metal dopants	Particle size (nm)	Phase	BET surface area (m ² /g)	Reference
P	0.020	Hydrothermal	TNBT	H ₃ PO ₂	14.50	Anatase	104.00	[67]
	0.140	Sol gel	TiO ₂ Degussa P25	H ₃ PO ₄	8.60	Anatase/rutile	154.00	[68]
N	0.265	Hydrothermal	TiO ₂ Degussa P25	TEA	15.40	Anatase/rutile	—	[69]
	1.600	Hydrothermal	TTIP	CH ₃ CH ₂ NH ₂	25.40	Anatase	—	[70]
S	1.500	Hydrothermal	TiCl ₄	CS(NH ₂) ₂	30.00	Anatase	—	[71]
	2.800	Hydrothermal	TiS ₂	TiS ₂	2.80	Anatase	—	[72]

the optical properties of TiO₂ photocatalysts [77]. Accordingly, different halogen dopants including iodine (I), bromine (Br), and fluorine (F) have been investigated in order to improve the morphology and the photocatalytic performance of TiO₂. A list of physical-chemical properties of metalloid-and halogen-doped TiO₂ and their advantages are given in Table 3.

Fluorine (F) has been doped into TiO₂ to increase the percentage of the anatase phase [78]. The substitution of F atoms and oxygen (O) atoms in TiO₂ lattice forms ≡Ti-F bond which has strong electron-withdrawing ability that prevents the recombination of photogenerated electron-hole pairs. However, some researchers have raised concern that beyond an optimal doping rate (F concentration > 0.5%), fluorine no longer acts as a mediator of interfacial charge transfer but serves as a recombination center [79]. The pH character of fluorine precursors plays an important role in determining the crystalline phase of photocatalyst formed. Basic fluorine precursors favor the formation of pure anatase phase TiO₂, whereas acidic fluorine precursors favor the formation of rutile/anatase or pure rutile phase TiO₂. On the other hand, fluorine was reported that it has no effect on the changes of band gap width [80]. Xu et al. [81] reported that the fluorine-doped TiO₂ prepared by hydrolysis process can improve the crystallinity as well as inhibit the grain growth of photocatalyst. Instead of this, fluorine doping can enhance the formation of hydroxyl groups on the titania surface, and thus, increase the phenol photodegradation rate.

Iodine is used to enhance the surface properties as well as the optical properties of TiO₂. Iodine is an effective dopant in shifting the absorption spectra of TiO₂ from UV light region to visible light region and facilitating the charge separation. The presence of iodine can also narrow the band gap of I-TiO₂, and hence improve the absorption ability of photocatalyst in the visible light region [88]. The red-shift of the band edge of iodine-doped TiO₂ is related to the formation of Helmholtz potential on the surface of TiO₂ with the presence of iodine. The presence of iodine facilitates the reduction of TiO₂ band gap energy from 3.2 eV to 3.0 eV and thus extends the photo-response region of I-TiO₂ to the visible light region [90]. This phenomenon was due to the shifting of the electron configuration of elements where I 5p

states mix with Ti 3d while O 2p moves to high energy region [91]. Wang et al. [89] successfully prepared single anatase phase of iodine-doped TiO₂ using hydrothermal method and they also showed that the iodine dopants hindered the growth of crystal particles by enhancing the energy barrier mutual diffusion between grains. From their results, the existence of iodine mainly improved the photosensitivity of the photocatalyst, broadened the visible light range, and decreased the band gap energy of TiO₂. Iodine dopants were proven to increase the formation of surface hydroxyl groups and thus improve the photocatalytic activity of TiO₂ [90]. However, beyond an optimal doping rate, iodine dopants serve as recombination centers for the charge carriers and hence inhibit the photocatalytic activities of the doped TiO₂ [88].

Boron (B) is known as a metalloid compound, which can be termed either a metal or a nonmetal. Some researchers contend that boron inhibits the growth of TiO₂ crystalline and thus increases the surface area of B-doped TiO₂ as well as inducing the crystalline process [63]. The formation of anatase phase is also promoted by adding boron dopants in the formation of nano-doped-TiO₂. For example, Xu et al. [66] found that B increased the surface area of nano-doped-TiO₂ by controlling the growth of TiO₂. Lu et al. [92] synthesized B-TiO₂ with the mixture of anatase and brookite phase by sol gel method. The foregoing notwithstanding, there are other researchers who are of the view that boron inhibits the transformation of amorphous phase to anatase phase. For instance, Zaleska et al. [82] found that no anatase phase was formed in the formation of boron-doped TiO₂ using sol gel method. Grabowska et al. [83] found out that boron-doped TiO₂ had lower surface area as compared to undoped TiO₂. One of the important features in boron doping is the red shift in the absorption band of TiO₂. The formation of Ti-O-B species enables the B-TiO₂ active in phenol photodegradation under visible light irradiation [82]. The incorporation of boron atoms into TiO₂ matrix by occupying O sites to form O-Ti-B induced the visible light photocatalytic activity of B-TiO₂ [92]. However, beyond an optimal doping rate, diboron trioxide phase (B₂O₃) was formed in the doped TiO₂, which led to lower the photocatalytic activity [82].

TABLE 3: Properties of metalloid or halogen-doped TiO₂ photocatalysts under various conditions.

Type of dopant	(Metal dopant/TiO ₂) molar ratio	Preparation of doped TiO ₂	Starting material of TiO ₂	Starting material of dopants	Crystallite size (nm)	Phase	BET surface area (m ² /g)	Reference
Metalloid								
B	0.001	Hydrothermal	Ti(OBu) ₄	NaBH ₄	2.59	Anatase	268.31	[63]
	9.000	Sol gel	Ti(OBu) ₄	VO(OPr) ₃	6.00	Anatase	127.00	[66]
	0.040	Sol gel	TTIP	H ₃ BO ₃	—	Anatase	219.00	[82]
	0.148	Sol gel	TiO ₂	(C ₂ H ₅ O) ₃ B	7.00	Anatase	192.00	[83]
Si	0.111	Destabilization	HFTA	HFSA	6.50	—	155.00	[84]
	0.030	Hydrothermal	Ti(OC ₄ H ₉) ₄	(C ₂ H ₅) ₄ SiO ₄	8.20	Anatase	191.70	[85]
	0.150	Templating	TBOT	TEOS	10.00	Anatase	120.00	[86]
Halogen								
F	0.050	Hydrothermal	Ti(OC ₃ H ₇) ₄	NH ₄ F	—	Anatase	48.00	[75]
	0.500	Hydrothermal	TBOT	NH ₄ HF ₂ -H ₂ O	11.20	Anatase	122.00	[77]
	0.770	Hydrothermal	TIP	NaF	10.00	Anatase	148.00	[78]
	0.039	Sol gel	Ti(C ₂ H ₅ O) ₄	CF ₃ COOH	13.20	Anatase	—	[80]
	0.190	Spray pyrolysis	H ₂ TiF ₆	H ₂ TiF ₆	—	Anatase	27.10	[87]
	0.001	Sol gel	Ti(OBu) ₄	NH ₄ F	3.78	Anatase	169.48	[81]
I	0.033	Hydrothermal	TTIP	HIO ₃	5.50	Anatase/brookite	137.60	[88]
	0.117	Hydrothermal	TNBT	KI	4.46	Anatase	184.87	[89]
	0.025	Sol gel	Ti(OBu) ₄	HIO ₃	5.50	Anatase	259.10	[90]

Silicon is another common metalloid used to dope TiO₂. Silicon dopants were proven to increase the thermal stability of anatase as well as suppress the anatase-to-rutile phase transformation [86]. Estruga et al. [84] studied the effect of silicon dopant on the formation of TiO₂ nanopowders. It was reported that the incorporation of silicon did not affect the crystalline phase or TiO₂ optical properties as compared to undoped TiO₂. However, silicon doping did increase the surface area of doped-TiO₂ with respect to undoped powders. In other study on the effects of the silicon dopants [85], Si-TiO₂ of smaller crystal size, larger pore volume and surface area, and single anatase phase was successfully synthesized using hydrothermal method. Meanwhile, the presence of Ti-O-Si bonds preserved high surface hydroxyl group concentrations, which influenced the subsequent photocatalytic activity of TiO₂. The nature behaviors of silicon metalloid can easily produce the hybridization bands in both valence and conduction bands which are beneficial in increasing the photogenerated charge carriers. Furthermore, the silicon doping can also reduce the band gap energy of TiO₂ and broaden the absorption spectra of TiO₂ [93].

3.4. Effect of Codoping. In order to further improve the morphology of TiO₂, the co-doping technique with double metal dopants, double nonmetal dopants, and double metal-nonmetal dopants has gained wide attention. Co-doped TiO₂ shifts the absorption edge of TiO₂ successfully from ultraviolet region to visible light region. The co-doping technique also improves the physical properties of the TiO₂ such as specific surface area and crystallite size while it sustains the phase transformation of anatase to rutile phase

[94]. Improved performance of TiO₂ under visible light is achieved up to an optimal doping level, after which performance deteriorates when the dopants become recombination centers for photogenerated electron-hole pairs [95].

A variety of rare metal dopants, including niobium (Nb), tungsten (W) and samarium (Sm) have been used in the co-doping technique by several researchers [96–98]. As with the other classes of dopants, Nb prevents the recombination of free electron and energized hole and extends the wavelength of absorbance of TiO₂ to increase its functionality. [97]. Ti atoms have been replaced with W atoms to form W–O–Ti bonds, which can induce the formation of the anatase phase as well as act as electron traps to suppress the recombination of energized holes and free electrons. Similar to other dopants, an excess of W levels decreases the performance of TiO₂. W is deposited on the surface of TiO₂ to blue-shift the absorption edge, thus increasing the band gap energy of TiO₂ under visible light [98]. Sm is also used to dope into TiO₂, which again restrains the phase transformation of the anatase phase to solid form and also stabilizes it in the final product. It also prevents the growth of the crystallite size of TiO₂ [96].

In the co-doping technique, the functions of metal dopants are generally to facilitate the charge separation of free electrons and energized holes and to decrease their recombination [97–99]. On the other hand, the functions of nonmetal dopants are generally to shift the absorption region of TiO₂ from the UV light region to the visible light region, besides narrowing the band gap of TiO₂ [100–102]. For example, Cu is applied in the co-doping technique to slow the growth of crystallite size of the TiO₂ by forming a complex with oxygen on the surface of TiO₂. At the same

TABLE 4: Properties of codoped-TiO₂ catalysts under various conditions.

Type of dopants used(x,y)	Optimum molar ratio of the dopants (M _x :M _y)	Codoped TiO ₂ preparation method	Starting material of TiO ₂	Starting material of co-dopants	Particle size (nm)	Phase	BET surface area (m ² /g)	Reference
F, N	1.00	Sol gel	TTIP	NH ₄ F, NH ₄ Cl	—	Anatase	102.00	[74]
Sm, N	1.50	Coprecipitation	Ti(SO ₄) ₂	Sm(NO ₃) ₃ , NH ₃	8.80	Anatase/Rutile	170.00	[96]
Fe, Nb	0.12	Sol gel	TTIP	Fe(NO ₃) ₃ •9H ₂ O, C ₄ NH ₄ NbO ₉ •10H ₂ O	10.00	Anatase	120.20	[97]
W, N	1.60	Hydrolysis	TiCl ₄	(NH ₄) ₂ WO ₄	11.00	Anatase	80.00	[98]
B, Fe	3.00	Sol gel	Ti(OBu) ₄	H ₃ BO ₃ , Fe(acac) ₃	12.00	Anatase	60.00	[99]
N, S	1.00	Hydrolysis	Ti(SO ₄) ₂	NH ₃ •H ₂ O, Ti(SO ₄) ₂	38.20	Anatase	56.10	[100]
S, I	1.00	Sol gel	TIP	Thiourea, HIO ₃	8.80	Anatase	85.00	[101]
N, S	33.33	Hydrothermal	Ti(SO ₄) ₂	CH ₄ N ₂ S, Ti(SO ₄) ₂	16.20	Anatase	—	[102]
Cu, S	2.00	Sol gel	TIP	CuCl ₂ •2H ₂ O, Thiourea	8.00	Anatase	—	[103]
F, N	1.00	Sol gel	TiCl ₄	NH ₄ F	11.90	Anatase	160.70	[104]
Pt, Cu	12.50	Impregnation	Titanium Tetraisobutyloxiide	H ₂ PtCl ₆ , Cu(NO ₃) ₂	8.90	Anatase	105.90	[105]
Fe, C	0.57	Sol gel/Solvothermal	Tetrabutyl titanate	Fe(NO ₃) ₃ •9H ₂ O	10.80	Anatase	158.00	[106]
Pt, N	0.02	Sol gel	TTIP	H ₂ PtCl ₆ , NH ₂ CONH ₂	5.00	Anatase	72.50	[107]
Cr, W	2.00	Pyrolysis	Ti ₂ (C ₂ O ₄) ₃ •10H ₂ O	(NH ₄) ₂ Cr ₂ O ₇ , Dimethylammonium tungstate	30.00	Anatase	60.00	[108]

time, Cu also prohibits the phase transformation from the anatase phase to the rutile phase [103]. carbon (C) and iodine (I) are similarly used as dopants to improve the performance and properties of TiO₂ [101].

The co-doping technique generates synergistic effects which enhance the properties of the final TiO₂ product [74, 96–109]. For example, when W and N are co-doped to TiO₂, the excited electrons are easily transferred from valence band into the new conduction band due to the narrowing of the band gap difference, while the recombination of free electrons and holes are not permitted [98]. Livraghi et al. [74] researched the effects of the co-doping technique using F and N on the formation of TiO₂. F could activate the active site of N by producing extra electrons to the low energy orbital of N_b^{*}. Doping with F and N created a synergism in which F improved the incorporation of N dopant into TiO₂.

Hamadianian et al. [103] showed that the use of Cu and S could form co-doped TiO₂ with TiO₂ displaying high performance under visible light irradiation. In this instance, Cu shifted the absorption range of TiO₂ from the UV region to the visible light region, while S lowered the band gap energy of TiO₂ by mixing its electron orbital with the O 2p orbital.

Overall, the co-doping technique is an effective method to improve the performance of TiO₂. A list of physical-chemical properties of co-doped TiO₂ and its advantages is given in Table 4. Three main benefits of co-doping are (1) high percentage of the anatase phase can be obtained, (2) phase transformation of the anatase phase to the rutile

phase is inhibited, and (3) small crystallite size and high specific surface area of TiO₂ are obtained [74, 96–109].

4. Effect of the Presence of Dopants on the Photocatalytic Degradation of Organic Pollutants

Various attempts at metal doping, nonmetal doping, and co-doping have been made to limit the recombination of the photogenerated electron-hole pairs in photocatalysis. Generally, doped TiO₂ performs better in the degradation of organic pollutants as compared with pure TiO₂ due to the modifications of the physical and chemical properties of TiO₂. In terms of physical properties, the doped TiO₂ has smaller crystallite size, larger specific surface area, and higher proportion of the anatase phase. The smaller crystallite size of doped TiO₂ reduces the likelihood of energized holes and free electron recombining, while the photocatalytic activity of TiO₂ is furthered enhanced by the charge carrier space distance being increased. Ma et al. [96] stated that dopants played an important role in the photocatalysis to create a charge space carrier region on the surface of TiO₂ that prevents the recombination of electron-hole pairs. The photodegradation process takes place on the surface of the photocatalyst, and a larger specific surface area makes available more active sites on the catalyst surface that increases the photodegradation potential of the photocatalyst [49, 66, 69, 70, 98, 106].

TABLE 5: Comparison on the photocatalytic degradation rate of different organic pollutants between pure TiO₂ and doped TiO₂.

Dopant(s)	Light source	Organic pollutant	Initial pollutant concentration (mg/L)	Irradiation time (h)	Degradation efficiency (%)		Reference
					Doped TiO ₂	Pure TiO ₂	
Fe	Visible light	Malachite green	5.00	1.00	78	63	[49]
	Visible light	Yellow XRG dye	100.00	8.00	37	18	[50]
	Visible light	Methyl orange	20.00	6.00	70	50	[53]
	UV light	Dichloromethane	96.00 ± 3.00	2.00	88	82	[54]
Pt	UV light	Methyl orange	20.00	1.50	98	90	[58]
		Acid green 16	1.20	1.00	100	98	[57]
Ce	UV light	Rhodamine B	0.50	2.00	80	98	[62]
B	Visible light	4-chlorophenol	50.00	4.00	78	20	[63]
	UV light	Methylene blue	19.00	4.00	98	78	[66]
Cu	Visible light	Methylene orange	10.00	0.75	100	70	[103]
F	UV light	Methylene blue	8.00	1.00	92	30	[79]
N	Visible light	Methylene orange	20.00	1.00	14	1	[76]
S	Visible light	4 chlorophenol	0.32	6.00	88	5	[70]
	UV light	Methylene orange	20.00	1.67	98	70	[69]
S, I	Visible light	Methylene blue	8.00	4.00	90	20	[101]
W, N	UV light	Phenol	60.00	4.00	93	83	[98]
Sm, N	Visible light	Salicylic acid	50.00	5.00	65	3	[96]
Fe, C	Visible light	Acid orange 7	50.00	5.00	90	8	[106]

Dopants narrow the band gap of the photocatalysts and enhance their photocatalytic abilities by shifting their photocatalytic activity from the ultra violet region to the visible light region. For example, Hamadani et al. [103] reported that Cu and S could alter the optical absorption wavelength of TiO₂ from UV light to visible light and hence lower the band gap of TiO₂ through the combination of electron orbital between S and O, respectively.

The photocatalytic activity of TiO₂ can be improved when chemical properties of doped TiO₂ are altered. Free electron and energized holes are the most important species in photocatalysis as hydroxyl radical can be produced from the energized holes during the reaction between water and the energized holes [79, 103]. The addition of dopants elevates TiO₂ efficiency by reducing the recombination of energized holes and free electrons. This accelerates the formation of hydroxyl radicals to speed up the photodegradation process [57, 106]. When Fe is used as a dopant, for example, the stable form of Fe³⁺ can be oxidized or reduced to form Fe²⁺ and Fe⁴⁺. Hence, Fe with its d orbital can act as intermediate for both energized holes and free electrons transfer. This speeds up the degradation of organic pollutants by preventing the recombination of energized holes and free electrons. Fe also lowers the conduction band energy and increases the valence band energy of TiO₂. The end result is the enhancement of photodegradation efficiency under visible light [49, 50, 53, 54].

In short, dopants can act as active sites for pollutant adsorption to facilitate the photodegradation reaction [96]. However, excessive amounts of dopants can retard the photocatalysis process. They reduce the opportunity of oxygen photoadsorbed on the surface of TiO₂ to react with free

electrons to form O₂⁻ or the corresponding hole to form •OH. Excess amounts of dopants deposited on surface of TiO₂ also increase the recombination rate of free electrons and energized holes, thus inhibiting the photodegradation process [57].

A summary of various dopants of TiO₂ applied in photocatalysis for the removal of organic pollutants is given in Table 5, which also compares the degradation efficiency between doped TiO₂ and pure TiO₂. Overall, dopants improve the performance of pure TiO₂ in the degradation of organic pollutants under visible light irradiation. They narrow the band gap of TiO₂ by shifting the optical absorption wavelength of TiO₂ from UV light to visible light.

5. Operational Factors Affecting the Photocatalytic Degradation

Based on the critical analysis of the existing researchers on the photocatalytic degradation of the organic pollutants, the important operating parameters affecting the efficiency of the photocatalytic degradation process are selected and discussed as follows: calcination temperature of nano-doped-TiO₂, initial concentration of photocatalyst, initial concentration of the reactant, and initial concentration of dopant dosing.

5.1. Effect of Calcination Temperature of Nano-Doped-TiO₂. Calcination process is commonly applied in the formation of TiO₂ photocatalyst as it can enhance the photocatalytic activity of photocatalyst. Deng et al. [46] studied the effect of calcination temperature on the photocatalytic performance of Fe-TiO₂. As shown in their results, the calcined Fe-TiO₂

TABLE 6: Effect of calcination temperature of nano-doped-TiO₂ on the photocatalytic degradation process.

Type of dopant	Doped TiO ₂ preparation method	Doped TiO ₂ loading (g/L)	Range of calcination temperature (°C)	Optimum calcination temperature (°C)	Organic pollutant	Initial pollutant concentration (mg/L)	Light source	Degradation efficiency, %	Reference
Fe	Sol gel	5.0	200–400	400	Methyl orange	20	UV-vis	99.7	[46]
Pt	Photochemical reduction	2.0	110–500	110	Methyl orange	20	UV	87.8	[58]
I, F	Sol gel-impregnation	1.0	500–700	500	Methylene blue	10	Sunlight	98	[94]
Sm, N	Coprecipitation	1.0	300–600	400	Salicylic acid	50	Visible light	67	[102]
Fe	Sol gel	1.0	0–900	500	Reactive blue 4	70	Ultrasonic	82	[110]
N, S	Hydrolysis	0.02	400–800	500	Formaldehyde	350	Sunlight	65	[100]
Cu, S	Sol gel	1.0	500–850	500	Methyl orange	10	Visible	100	[103]
Pt, Cu	Impregnation	1.0	300–700	300	Nitrate	10	UV	90	[105]
Pr	Sol gel	1.0	100–800	600	Phenol	50	UV	96	[111]
KOX	Sol gel	1.0	.0–1000	800	Methylene blue	20	Fluorescence blacklight	100	[112]

showed higher photocatalytic activity compared to that Fe-TiO₂ formed in the absence of calcination process. It was attributed to the formation of anatase phase from titanate.

However, beyond the optimum calcination temperature, the photocatalytic activity of photocatalyst is observed to decrease due to the agglomeration and sintering damage of Fe-TiO₂ at high temperature [94]. Huang et al. [58] studied the effect of calcination temperature on the photocatalytic activity of Pt-doped TiO₂. Based on their results, the calcined Pt-TiO₂ was confirmed to have higher efficiency and activity in the photocatalytic degradation of pollutant up to certain optimum calcination temperature. Beyond the optimum calcination temperature, the photocatalytic activity was observed to decrease due to the agglomeration of particles which reduce the specific surface area of the photocatalyst.

Calcination process can influence the surface area, morphology, and crystallinity of the prepared photocatalyst. Ma et al. [96] synthesized and calcined the co-doped Sm/N-TiO₂ at different temperatures. The prepared photocatalysts were tested on the photodegradation of salicylic acid under visible light irradiation. They found out that calcination process improved the crystallinity, particle size, and surface area of photocatalyst as compared to undoped photocatalysts.

The calcination temperature affects greatly the optical absorption of the photocatalysts. High calcination temperature can promote the replacement of nitrogen by oxygen in the air. Consequently, the absorption of photocatalyst in the visible light region decreases, and hence, decreasing the photocatalytic activity of TiO₂. Many researchers have confirmed that the calcination process is important in the formation of doped TiO₂ and that the properties of photocatalyst such as surface area and crystallinity of doped TiO₂ are strongly dependent on the calcination temperature [100, 103, 110]. With further increase in the calcination temperature, the surface area of TiO₂ started to decrease

as well as the transformation of anatase to rutile phase, and thus, the photocatalytic activity of TiO₂ decreased. Li et al. [105] studied the effect of calcination temperature on benzene photodegradation using Pt/Cu-TiO₂. They also agreed that high calcination temperature produced low specific surface area, large particle size, and low crystallinity phase of the agglomerated doped-TiO₂. Subsequently, the less active site eventually lowers the photocatalytic activity of TiO₂.

Suwanchawalit and Wongnawa [112] studied the photodegradation of methylene blue using potassium oxalate-doped TiO₂. Based on their result, noncalcined samples have high specific surface area but low percentage of anatase phase in the TiO₂. These resulted that non-calcined samples showed higher adsorptive capacity but lower photocatalytic activity as compared to calcined samples. As the calcination temperature increases, the adsorptive property of photocatalyst decreases with increasing the photocatalytic activity. In addition, the optimum calcination temperature provides the moderate adsorptive capacity and excellent photocatalytic activity of the photocatalysts. On the other hand, further increase of calcination temperature decreases the photocatalytic performance of photocatalyst. Kemp and McIntyre [113] studied the photodegradation of poly(vinyl chloride) using V-TiO₂ and reported that lower calcination temperature samples showed better photodegradation rate compared to that sample produced at high calcination temperature (1000°C).

Table 6 summarizes the effect of calcination temperatures of nano-doped-TiO₂ on the photocatalytic degradation of various organic pollutants. The table reveals that different optimum calcination temperatures have been reported by different researchers. Such differences in the preparation and posttreatment conditions contribute different morphology of nano-doped-TiO₂.

TABLE 7: Effect of initial organic pollutant concentration on the photocatalytic activity of nano-doped-TiO₂.

Type of dopant	Doped TiO ₂ preparation method	Doped TiO ₂ loading (g/L)	Organic pollutant	Range of pollutant concentration (mg/L)	Optimum pollutant concentration (mg/L)	Light source	Irradiation time (h)	Degradation efficiency (%)	Reference
Ag	Sol gel	1	Crystal violet	10–80	10	UV	1.75	100	[115]
Ba	Sol gel	0.2	4-chlorophenol	50–300	250	UV	—	100	[10]
C	Sol gel	1	Methylene blue	5–50	5	Solar light	2/3	100	[116]
Ce	Coprecipitation	4	Phenol	1000–5000	1000	UV	2	100	[117]
Fe	Sol gel	1.5	Reactive blue 4	70–120	70	Ultrasonic	1	92	[110]
N	Sol gel	0.4	Phenol	10–200	20	UV	—	—	[118]
P	Sol gel	0.2	Rhodamine B	5–50	12	Solar light	—	85	[119]
Pr	Sol gel	1	Phenol	12.5–200	25	UV	1	100	[111]
W	Liquid phase deposition	—	Dodecyl-benzenesulfonate	250–100	250	Visible	1.5	98	[120]
Zr	Sol gel	0.2	4-chlorophenol	50–300	250	UV	—	100	[121]

5.2. Effect of Initial Reactant Concentration. The influence of initial reactant concentration on the photocatalytic degradation is a great aspect of the study. The relationship between initial reactant concentration and photocatalytic activity of TiO₂ is associated with the adsorption of reactant on the surface of photocatalyst and the screening effect due to overloading of reactant [110]. In general, it is found that the photocatalytic activity of the photocatalysts decreases with increasing the initial reactant concentration. This may be due to the limitation of the numbers of active sites of photocatalyst available on the photocatalyst surface. On the other hand, Andronic et al. [114] reported that the photodegradation efficiency decreased when initial reactant concentration increased. This is due to the decrease of the path length of the photon when entering the reactant solution, with direct consequence on the formation of electron-hole pairs.

In other study on the effect of initial reactant concentration [117], the adsorption of phenol intermediates could lead to the irreversible deposition on the surface of Ce-TiO₂ photocatalyst and thus reduce the photodegradation efficiency. Meanwhile, the excessive of reactant concentration could lead to the screening effect that prohibited the penetration of light irradiation [121]. Beyond the optimum concentration of reactant, more reactant molecules will adsorb on the photocatalyst surface, prohibiting the absorption of photon to form charge carriers. Otherwise, it will also prevent the excessive adsorption of reactant on the active sites of the photocatalyst, inhibit the generation of hydroxyl radical and hence decrease the photocatalytic activity of the photocatalyst [110].

Table 7 summarizes the effect of initial reactant concentration on the photocatalytic degradation of various organic pollutants.

5.3. Effect of Photocatalyst Dosage. The effect of photocatalyst dosage on the photocatalytic degradation process has been widely studied. The reason generally advanced for this is that

the optimum photocatalyst dosage maximizes the photocatalytic performance and minimizes the cost and energy.

In most of the studies, the increase in the photocatalyst dosage increases the number of photons absorbed on the photocatalyst surface, which in turn increases the generation of electron/hole pairs and increases the number of hydroxyl radicals. The increase in the photocatalyst dosage also increases the number of organic pollutant adsorbed on the surface of photocatalyst and facilitates the photocatalytic activity [111, 122].

However, when the photocatalyst dosage increases above the optimum level, the photocatalytic activity decreases, which is due to the shadowing effect and the penetration depth of light irradiation by the high turbidity suspension [116]. Huang et al. [58] added that as the excess catalyst prevent the penetration of light in the photocatalytic degradation process, the light scattering and the screening effect decreased among the photocatalyst particles and the efficiency of the photocatalytic degradation reduced accordingly. Furthermore, the increase of the photocatalyst dosage beyond the optimum level may result in the deactivation of the catalyst particle and the collision between the active molecules and ground state molecules of titania [10] and hence degradation rate decrease.

Wang et al. [123] studied the effect of photocatalyst amount on the photocatalytic activity of the catalyst. Based on the result obtained, the photocatalytic degradation was significantly affected by the photocatalyst dosage and that the optimal photocatalyst dosage was 1000 mg/L. When in excess, existence of dopant on the particle surface of TiO₂ lessens the active sites on the surface of TiO₂, aids the agglomeration TiO₂, and thus hinders the photocatalytic activity.

There are several considerations affecting the optimum photocatalyst dosage on the photocatalytic degradation process. These include the type of dopants, light intensity, and initial reactant concentration. Thus, further study is still required to provide a complete understanding of the

TABLE 8: Effect of photocatalyst dosage on the photocatalytic activity of nano-doped-TiO₂ in the photocatalytic degradation of various organic pollutants.

Type of dopant	Doped TiO ₂ preparation method	Range of photocatalyst dosage (g/L)	Optimum photocatalyst loading (g/L)	Organic pollutant	Initial pollutant concentration (mg/L)	Light source	Irradiation time (h)	Degradation efficiency (%)	Reference
Sn	Sol gel/dip coating	5–15	12.5	Orange-G	50	UV	1	99.1	[122]
Zr	Sol gel	100–500	2.0	4-chlorophenol	250	UV	—	—	[121]
Ba	Sol gel	100–500	2.0	4-chlorophenol	250	UV	—	—	[10]
Fe	Hydrothermal	0.25–1.25	1.0	Azo fuchsine	10	Ultrasonic	1	60	[123]
	Sol gel	0.5–2.0	1.5	Reactive Blue 4	70	Ultrasonic	1	90	[110]
Ag	Photo reduction	326–2608	3.0	Direct Red 23	326	UV	2.5	55	[124]
C	Sol gel	0.5–4.0	1.0	Methylene blue	10	Solar light	1.67	100	[116]
P	Sol gel	0.2–1.2	0.4	Rhodamine B	12	Sunlight	4	93	[119]
Pt	Sol gel	0.0–1.2	1.0	Phenol	50	UV	2	96.5	[111]
	Sol gel	0.5–6.0	3.0	Methyl orange	20	UV	0.5	90.5	[58]

relationship between photocatalyst dosage and other parameters. Table 8 shows the effect of photocatalyst dosage on the photocatalytic degradation of various organic pollutants.

5.4. Effect of Dopant Concentration. Dopant concentration on the photocatalytic activity of photocatalysts has been investigated. The photocatalytic activity was found to be directly proportional to the dopant concentration. However, it was noticed that above a certain level of concentration, the photocatalytic performance decreases.

In Deng et al.'s research [46], the increasing rate of the photocatalytic degradation slowed down when the dopant concentration of Fe was higher than 0.5%. This indicated that Fe³⁺ ions acted as photogenerated electron trap, so the recombination of hole-electron pairs was inhibited. Meanwhile, the transfer of electron from Fe²⁺ to Ti⁴⁺ surface due to the proximity of the energy levels was also one of the factors in enhancing photocatalytic activity. This is in agreement with recent reports [50, 53, 55]. Zhu et al. [50] also reported an enhancement degradation rates for Fe-doped TiO₂ prepared by hydrothermal treatment as compared to undoped TiO₂ in the photodegradation of active yellow XRG. Tong et al. [53] and Ambrus et al. [55] reported an improved photocatalytic performance for the optimum Fe dopant concentration. Beyond the optimum concentration of dopant, the photodegradation rate decreased.

On the other hand, noble metals such as Pt, Au, and Pd are always advantageous to the photocatalytic degradation process. Sakthivel et al. [57] studied the effect of dopant concentration on the photocatalytic degradation of acid green 16 using doped TiO₂. In their research, the optimum dopant loading concentration enhanced the photocatalytic activity by increasing the photonic efficiency and inhibiting the electron-hole pair recombination. However, any further

increase in dopant content exert is negative effect on the photocatalytic activity of the photocatalyst. When in excess, the existence of dopant on the TiO₂ surface blocks the active sites of TiO₂, lessens the adsorption of reactant, and, thereby, reduces the photodegradation efficiency. Huang et al. [58] also studied the decolorization performance of methyl orange using Pt-doped TiO₂. They observed that there was a great enhancement in the decolorization by doping TiO₂ with different amount of wt% Pt. Their report showed that a doping level beyond the optimum doping level (1.5 wt% Pt) seemed to affect adversely the photocatalytic activity. Any further increase in dopant concentration could notably induce the photogenerated hole and electron recombination and decrease the photocatalytic efficiency.

The effect of halogen doping on the photocatalytic degradation of organic pollutants in TiO₂ aqueous solutions has been investigated [77]. They have concluded that F has a strong enhancing effect on the photocatalytic activity, by altering the properties of TiO₂ such as crystallite size, crystallinity, and phase structure. They noted that the addition of F⁻ ions promotes the formation of anatase phase by suppressing the formation of brookite phase, subsequently forms ≡Ti-F groups, and hence, enhances the free •OH radicals production and reduces the photogenerated electron-hole recombination.

Yu et al. [79] studied the effect of sulfur dopant amount in the photocatalytic activity of S-doped TiO₂. The photocatalytic degradation of methyl orange was studied in the presence of S-doped TiO₂. In their research, they have found that the optimum loading of S dopants could produce TiO₂ with smaller particle size and larger surface area, which increases the formation of photogenerated electrons and thus increases the photocatalytic activity.

The foregoing notwithstanding, there are other researchers who are of the view that the presence of dopant

TABLE 9: Effect of dopant amount on the photocatalytic activity of nano-doped-TiO₂ in the photocatalytic degradation of various organic pollutants.

Type of dopant	Doped TiO ₂ preparation method	Range of dopant amount (wt%)	Optimum dopant concentration (wt%)	Organic pollutant	Initial reactant concentration (mg/L)	Light source	Irradiation time (h)	Degradation efficiency (%)	Reference
Fe	Sol gel	0.0–1.0	0.500	Methyl orange	20.0	UV-vis	3.0	99.7	[46]
	Hydrothermal	0.00–0.12	0.090	XRG	100.0	UV	7.0	42	[50]
	Controlled hydrolysis	0.00–0.20	0.200	Methyl orange	20.0	UV	6.0	72	[53]
	Co-precipitation	0.0–10.0	0.017	Phenol	18.8	Visible	3.1	20	[55]
Pt	Hydrothermal	0.0–5.0	0.001	Methylene blue	100.0	UV	1.0	72	[51]
	Impregnation	0.0–1.6	0.800	Acid green 16	122.0	UV	1.0	94	[57]
	Photochemical reduction	0.0–3.0	1.500	Methyl orange	20.0	UV	0.5	88	[58]
Pd	Impregnation	0.0–2.0	0.050	Acid green 16	122.0	UV	1.0	80	[57]
Au	Impregnation	0.0–1.6	0.800	Acid green 16	122.0	UV	1.0	98	[57]
S	Hydrothermal	0.0–2.0	0.012	Methyl orange	20.0	UV	0.7	96	[79]
Ce	Hydrothermal	0.0–5.0	0.017	Rhodamine B	24.0	UV	2.0	90	[62]

is not requisite for the improvement of the photocatalytic activity of TiO₂. Li et al. [51] investigated the photocatalytic performance of Fe-doped TiO₂ in the degradation of methylene blue. In their research, they have found that the presence of Fe has a suppressing influence on the photocatalytic performance of TiO₂. The inhibition effect can be explained as the insertion of Fe³⁺ ions into the TiO₂ interior matrix, which behaved as charge carrier scavengers. Probably the isolated Fe³⁺ ions from the surface lower the chances of trapped charge carriers and increases the recombination rate of the photogenerated electron-hole pairs. Also, Xiao et al. [63] found that undoped TiO₂ showed better photocatalytic activity as compared to that Ce-doped TiO₂ in the Rhodamine B degradation. They have found that the presence of Ce has a suppressing influence on the photocatalytic performance of TiO₂. It can be explained that the partial blockage of the TiO₂ active sites lowered the activation of the TiO₂ catalyst particle and the collision between the active molecules and ground state molecules of TiO₂, and thus, decreasing the photocatalytic activity.

Table 9 shows the effect of dopant amount on the photocatalytic degradation of various organic pollutants.

6. Conclusions

A comprehensive series of nano-doped-TiO₂ photocatalysts are discussed in this paper. There are three main sections included: (a) the presence of various dopants (metal dopants, nonmetal dopants, halogen dopants, metalloid dopants, and co-dopants) in the formation of nano-doped-TiO₂ photocatalysts, (b) the effect of the presence of dopants on the

photocatalytic degradation of organic pollutants, and (c) the effects of various operating parameters on the photocatalytic degradation of organic pollutants in the presence of nano-doped-TiO₂ photocatalysts. Judging from the referenced literatures, doping techniques are simple procedures used to enhance photocatalysis by TiO₂. Desirable characteristics such as small crystallite size, high specific surface area, and the presence of the anatase phase are easily achieved by doping techniques. Nevertheless, the mechanisms underlying doped TiO₂ are still unclear. The relationship between the photocatalytic activity and physical properties of TiO₂ requires further study to arrive at optimal conditions for the photocatalytic degradation of various organic pollutants.

Acknowledgments

The authors gratefully acknowledge the Universiti Sains Malaysia and the Ministry of Science, Technology and Innovation of Malaysia for giving support and funding in the form of USM Fellowship, Research University Grant (1001/PJKIMIA/811068), and Postgraduate Research Grant Scheme (1001/PJKIMIA/8033051).

References

- [1] U. M. Gaya and A. H. Abdullah, "Heterogeneous photocatalytic degradation of organic contaminants over titanium dioxide: a review of fundamentals, progress and problems," *Journal of Photochemistry and Photobiology C*, vol. 9, no. 1, pp. 1–12, 2007.
- [2] A. Di Paola, G. Cufalo, M. Addamo et al., "Photocatalytic activity of nanocrystalline TiO₂ (brookite, rutile and

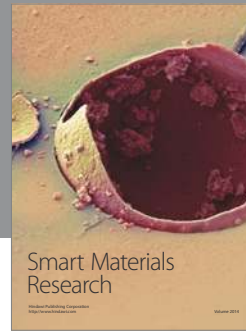
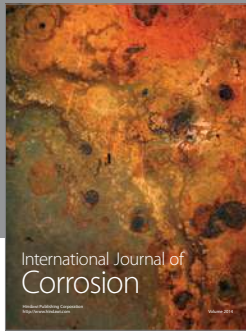
- brookite-based) powders prepared by thermohydrolysis of TiCl_4 in aqueous chloride solutions,” *Colloids and Surfaces A*, vol. 317, no. 1–3, pp. 366–376, 2008.
- [3] H. Yu, J. Yu, B. Cheng, and J. Lin, “Synthesis, characterization and photocatalytic activity of mesoporous titania nanorod/titanate nanotube composites,” *Journal of Hazardous Materials*, vol. 147, no. 1-2, pp. 581–587, 2007.
- [4] S. Nagamine, A. Sugioka, H. Iwamoto, and Y. Konishi, “Formation of TiO_2 hollow microparticles by spraying water droplets into an organic solution of titanium tetraisopropoxide (TTIP)—effects of TTIP concentration and TTIP-protecting additives,” *Powder Technology*, vol. 186, no. 2, pp. 168–175, 2008.
- [5] J. Yu, G. Wang, B. Cheng, and M. Zhou, “Effects of hydrothermal temperature and time on the photocatalytic activity and microstructures of bimodal mesoporous TiO_2 powders,” *Applied Catalysis B*, vol. 69, no. 3-4, pp. 171–180, 2007.
- [6] J. H. Lee and Y. S. Yang, “Effect of HCl concentration and reaction time on the change in the crystalline state of TiO_2 prepared from aqueous TiCl_4 solution by precipitation,” *Journal of the European Ceramic Society*, vol. 25, no. 16, pp. 3573–3578, 2005.
- [7] A. Verma, A. K. Bakhshi, and S. A. Agnihotry, “Effect of different precursor sols on the properties of CeO_2 - TiO_2 films for electrochromic window applications,” *Electrochimica Acta*, vol. 51, no. 22, pp. 4639–4648, 2006.
- [8] W. Zhang, L. Zou, and L. Wang, “Photocatalytic TiO_2 /adsorbent nanocomposites prepared via wet chemical impregnation for wastewater treatment: a review,” *Applied Catalysis A*, vol. 371, no. 1-2, pp. 1–9, 2009.
- [9] A. Orendorz, A. Brodyanski, J. Lösch et al., “Phase transformation and particle growth in nanocrystalline anatase TiO_2 films analyzed by X-ray diffraction and Raman spectroscopy,” *Surface Science*, vol. 601, no. 18, pp. 4390–4394, 2007.
- [10] N. Venkatachalam, M. Palanichamy, and V. Murugesan, “Sol-gel preparation and characterization of alkaline earth metal doped nano TiO_2 : efficient photocatalytic degradation of 4-chlorophenol,” *Journal of Molecular Catalysis A*, vol. 273, no. 1-2, pp. 177–185, 2007.
- [11] J. Y. Kim, C. S. Kim, H. K. Chang, and T. O. Kim, “Synthesis and characterization of N-doped $\text{TiO}_2/\text{ZrO}_2$ visible light photocatalysts,” *Advanced Powder Technology*, vol. 22, no. 3, pp. 443–448, 2011.
- [12] X. T. Zhang, K. Udagawa, Z. Y. Liu et al., “Photocatalytic and photoelectrochemical studies on N-doped TiO_2 photocatalyst,” *Journal of Photochemistry and Photobiology A*, vol. 202, no. 1, pp. 39–47, 2009.
- [13] D. Wu, M. Long, W. Cai, C. Chen, and Y. Wu, “Low temperature hydrothermal synthesis of N-doped TiO_2 photocatalyst with high visible-light activity,” *Journal of Alloys and Compounds*, vol. 502, no. 2, pp. 289–294, 2010.
- [14] D. G. Huang, S. J. Liao, J. M. Liu, Z. Dang, and L. Petrik, “Preparation of visible-light responsive N-F-codoped TiO_2 photocatalyst by a sol-gel-solvothermal method,” *Journal of Photochemistry and Photobiology A*, vol. 184, no. 3, pp. 282–288, 2006.
- [15] C. Wen, H. Deng, J. Y. Tian, and J. M. Zhang, “Photocatalytic activity enhancing for TiO_2 photocatalyst by doping with La,” *Transactions of Nonferrous Metals Society of China*, vol. 16, pp. s728–s731, 2006.
- [16] C.-H. Chang and Y.-H. Shen, “Synthesis and characterization of chromium doped SrTiO_3 photocatalyst,” *Materials Letters*, vol. 60, no. 1, pp. 129–132, 2006.
- [17] S. X. Liu and X. Y. Chen, “A visible light response TiO_2 photocatalyst realized by cationic S-doping and its application for phenol degradation,” *Journal of Hazardous Materials*, vol. 152, no. 1, pp. 48–55, 2008.
- [18] A. Kubacka, G. Colón, and M. Fernández-García, “Cationic (V, Mo, Nb, W) doping of TiO_2 -anatase: a real alternative for visible light-driven photocatalysts,” *Catalysis Today*, vol. 143, no. 3-4, pp. 286–292, 2009.
- [19] H. Cai, G. Liu, W. Lü, X. Li, L. Yu, and D. Li, “Effect of Ho-doping on photocatalytic activity of nanosized TiO_2 catalyst,” *Journal of Rare Earths*, vol. 26, no. 1, pp. 71–75, 2008.
- [20] E. Setiawati and K. Kawano, “Stabilization of anatase phase in the rare earth; Eu and Sm ion doped nanoparticle TiO_2 ,” *Journal of Alloys and Compounds*, vol. 451, no. 1-2, pp. 293–296, 2008.
- [21] K. Pirkanniemi and M. Sillanpää, “Heterogeneous water phase catalysis as an environmental application: a review,” *Chemosphere*, vol. 48, no. 10, pp. 1047–1060, 2002.
- [22] J. Nowotny, T. Bak, M. K. Nowotny, and L. R. Sheppard, “Titanium dioxide for solar-hydrogen I. Functional properties,” *International Journal of Hydrogen Energy*, vol. 32, no. 14, pp. 2609–2629, 2007.
- [23] J. A. Rengifo-Herrera, K. Pierzchala, A. Sienkiewicz, L. Forró, J. Kiwi, and C. Pulgarin, “Abatement of organics and *Escherichia coli* by N, S co-doped TiO_2 under UV and visible light. Implications of the formation of singlet oxygen ($^1\text{O}_2$) under visible light,” *Applied Catalysis B*, vol. 88, no. 3-4, pp. 398–406, 2009.
- [24] J. J. Carvajal, V. Nikolov, R. Solé et al., “Crystallization region, crystal growth, and characterization of rubidium titanil phosphate codoped with niobium and lanthanide ions,” *Chemistry of Materials*, vol. 14, no. 7, pp. 3136–3142, 2002.
- [25] P. Supphasirongjaroen, P. Praserttham, J. Panpranot, D. Naranong, and O. Mekasuwandumrong, “Effect of quenching medium on photocatalytic activity of nano- TiO_2 prepared by solvothermal method,” *Chemical Engineering Journal*, vol. 138, no. 1–3, pp. 622–627, 2008.
- [26] O. Carp, C. L. Huisman, and A. Reller, “Photoinduced reactivity of titanium dioxide,” *Progress in Solid State Chemistry*, vol. 32, no. 1-2, pp. 33–177, 2004.
- [27] A. Kudo, R. Niishiro, A. Iwase, and H. Kato, “Effects of doping of metal cations on morphology, activity, and visible light response of photocatalysts,” *Chemical Physics*, vol. 339, no. 1–3, pp. 104–110, 2007.
- [28] X. Wang, S. Meng, X. Zhang, H. Wang, W. Zhong, and Q. Du, “Multi-type carbon doping of TiO_2 photocatalyst,” *Chemical Physics Letters*, vol. 444, no. 4–6, pp. 292–296, 2007.
- [29] X. Fan, X. Chen, S. Zhu et al., “The structural, physical and photocatalytic properties of the mesoporous Cr-doped TiO_2 ,” *Journal of Molecular Catalysis A*, vol. 284, no. 1-2, pp. 155–160, 2008.
- [30] E. György, G. Socol, E. Axente, I. N. Mihailescu, C. Ducu, and S. Ciuca, “Anatase phase TiO_2 thin films obtained by pulsed laser deposition for gas sensing applications,” *Applied Surface Science*, vol. 247, no. 1–4, pp. 429–433, 2005.
- [31] D. S. Kim, S. J. Han, and S.-Y. Kwak, “Synthesis and photocatalytic activity of mesoporous TiO_2 with the surface area, crystallite size, and pore size,” *Journal of Colloid and Interface Science*, vol. 316, no. 1, pp. 85–91, 2007.
- [32] A. R. Liu, S. M. Wang, Y. R. Zhao, and Z. Zheng, “Low-temperature preparation of nanocrystalline TiO_2 photocatalyst with a very large specific surface area,” *Materials Chemistry and Physics*, vol. 99, no. 1, pp. 131–134, 2006.

- [33] W. Kongsuebchart, P. Praserttham, J. Panpranot, A. Sirisuk, P. Supphasrironjaroen, and C. Satayaprasert, "Effect of crystallite size on the surface defect of nano-TiO₂ prepared via solvothermal synthesis," *Journal of Crystal Growth*, vol. 297, no. 1, pp. 234–238, 2006.
- [34] M. Hirano, C. Nakahara, K. Ota, O. Tanaike, and M. Inagaki, "Photoactivity and phase stability of ZrO₂-doped anatase-type TiO₂ directly formed as nanometer-sized particles by hydrolysis under hydrothermal conditions," *Journal of Solid State Chemistry*, vol. 170, no. 1, pp. 39–47, 2003.
- [35] L. G. Devi, B. N. Murthy, and S. G. Kumar, "Photocatalytic activity of TiO₂ doped with Zn²⁺ and V⁵⁺ transition metal ions: influence of crystallite size and dopant electronic configuration on photocatalytic activity," *Materials Science and Engineering B*, vol. 166, no. 1, pp. 1–6, 2010.
- [36] M. S. Nahar, J. Zhang, K. Hasegawa, S. Kagaya, and S. Kuroda, "Phase transformation of anatase-rutile crystals in doped and undoped TiO₂ particles obtained by the oxidation of polycrystalline sulfide," *Materials Science in Semiconductor Processing*, vol. 12, no. 4–5, pp. 168–174, 2009.
- [37] G. Q. Li, C. Y. Liu, and Y. Liu, "Different effects of cerium ions doping on properties of anatase and rutile TiO₂," *Applied Surface Science*, vol. 253, no. 5, pp. 2481–2486, 2006.
- [38] C.-T. Hsieh, W.-S. Fan, W.-Y. Chen, and J.-Y. Lin, "Adsorption and visible-light-derived photocatalytic kinetics of organic dye on Co-doped titania nanotubes prepared by hydrothermal synthesis," *Separation and Purification Technology*, vol. 67, no. 3, pp. 312–318, 2009.
- [39] K. Suriye, P. Praserttham, and B. Jongsomjit, "Impact of Ti³⁺ present in titania on characteristics and catalytic properties of the Co/TiO₂ catalyst," *Industrial and Engineering Chemistry Research*, vol. 44, no. 17, pp. 6599–6604, 2005.
- [40] M. Atashfaraz, M. Shariaty-Niassar, S. Ohara et al., "Effect of titanium dioxide solubility on the formation of BaTiO₃ nanoparticles in supercritical water," *Fluid Phase Equilibria*, vol. 257, no. 2, pp. 233–237, 2007.
- [41] K. J. Zhang, W. Xu, X. J. Li, S. J. Zheng, G. Xu, and J. H. Wang, "Photocatalytic oxidation activity of titanium dioxide film enhanced by Mn non-uniform doping," *Transactions of Nonferrous Metals Society of China*, vol. 16, no. 5, pp. 1069–1075, 2006.
- [42] M. Wang, G. Song, J. Li, L. Miao, and B. Zhang, "Direct hydrothermal synthesis and magnetic property of titanate nanotubes doped magnetic metal ions," *Journal of University of Science and Technology Beijing*, vol. 15, no. 5, pp. 644–648, 2008.
- [43] R.-F. Chen, C.-X. Zhang, J. Deng, and G.-Q. Song, "Preparation and photocatalytic activity of Cu²⁺-doped TiO₂/SiO₂," *International Journal of Minerals, Metallurgy and Materials*, vol. 16, no. 2, pp. 220–225, 2009.
- [44] J.-C. Xu, M. Lu, X.-Y. Guo, and H.-L. Li, "Zinc ions surface-doped titanium dioxide nanotubes and its photocatalysis activity for degradation of methyl orange in water," *Journal of Molecular Catalysis A*, vol. 226, no. 1, pp. 123–127, 2005.
- [45] R. Janes, L. J. Knightley, and C. J. Harding, "Structural and spectroscopic studies of iron (III) doped titania powders prepared by sol-gel synthesis and hydrothermal processing," *Dyes and Pigments*, vol. 62, no. 3, pp. 199–212, 2004.
- [46] L. Deng, S. Wang, D. Liu et al., "Synthesis, characterization of Fe-doped TiO₂ nanotubes with high photocatalytic activity," *Catalysis Letters*, vol. 129, no. 3–4, pp. 513–518, 2009.
- [47] C. C. Tsai and H. Teng, "Chromium-doped titanium dioxide thin-film photoanodes in visible-light-induced waterli cleavage," *Applied Surface Science*, vol. 254, no. 15, pp. 4912–4918, 2008.
- [48] C.-G. Wu, C.-C. Chao, and F.-T. Kuo, "Enhancement of the photo catalytic performance of TiO₂ catalysts via transition metal modification," *Catalysis Today*, vol. 97, no. 2–3, pp. 103–112, 2004.
- [49] M. Asiltürk, F. Sayilkan, and E. Arpaç, "Effect of Fe³⁺ ion doping to TiO₂ on the photocatalytic degradation of Malachite Green dye under UV and vis-irradiation," *Journal of Photochemistry and Photobiology A*, vol. 203, no. 1, pp. 64–71, 2009.
- [50] J. Zhu, W. Zheng, B. He, J. Zhang, and M. Anpo, "Characterization of Fe-TiO₂ photocatalysts synthesized by hydrothermal method and their photocatalytic reactivity for photodegradation of XRG dye diluted in water," *Journal of Molecular Catalysis A*, vol. 216, no. 1, pp. 35–43, 2004.
- [51] Z. Li, W. Shen, W. He, and X. Zu, "Effect of Fe-doped TiO₂ nanoparticle derived from modified hydrothermal process on the photocatalytic degradation performance on methylene blue," *Journal of Hazardous Materials*, vol. 155, no. 3, pp. 590–594, 2008.
- [52] C. Adán, J. Carbajo, A. Bahamonde, and A. Martínez-Arias, "Phenol photodegradation with oxygen and hydrogen peroxide over TiO₂ and Fe-doped TiO₂," *Catalysis Today*, vol. 143, no. 3–4, pp. 247–252, 2009.
- [53] T. Tong, J. Zhang, B. Tian, F. Chen, and D. He, "Preparation of Fe³⁺-doped TiO₂ catalysts by controlled hydrolysis of titanium alkoxide and study on their photocatalytic activity for methyl orange degradation," *Journal of Hazardous Materials*, vol. 155, no. 3, pp. 572–579, 2008.
- [54] W. C. Hung, S. H. Fu, J. J. Tseng, H. Chu, and T. H. Ko, "Study on photocatalytic degradation of gaseous dichloromethane using pure and iron ion-doped TiO₂ prepared by the sol-gel method," *Chemosphere*, vol. 66, no. 11, pp. 2142–2151, 2007.
- [55] Z. Ambrus, N. Balázs, T. Alapi et al., "Synthesis, structure and photocatalytic properties of Fe(III)-doped TiO₂ prepared from TiCl₃," *Applied Catalysis B*, vol. 81, no. 1–2, pp. 27–37, 2008.
- [56] G. Colón, M. C. Hidalgo, J. A. Navío, E. P. Melián, O. G. Díaz, and J. M. Doña, "Influence of amine template on the photoactivity of TiO₂ nanoparticles obtained by hydrothermal treatment," *Applied Catalysis B*, vol. 78, no. 1–2, pp. 176–182, 2008.
- [57] S. Sakthivel, M. V. Shankar, M. Palanichamy, B. Arabindoo, D. W. Bahnemann, and V. Murugesan, "Enhancement of photocatalytic activity by metal deposition: characterisation and photonic efficiency of Pt, Au and Pd deposited on TiO₂ catalyst," *Water Research*, vol. 38, no. 13, pp. 3001–3008, 2004.
- [58] M. Huang, C. Xu, Z. Wu, Y. Huang, J. Lin, and J. Wu, "Photocatalytic discolorization of methyl orange solution by Pt modified TiO₂ loaded on natural zeolite," *Dyes and Pigments*, vol. 77, no. 2, pp. 327–334, 2008.
- [59] Y. Ishibai, J. Sato, T. Nishikawa, and S. Miyagishi, "Synthesis of visible-light active TiO₂ photocatalyst with Pt-modification: role of TiO₂ substrate for high photocatalytic activity," *Applied Catalysis B*, vol. 79, no. 2, pp. 117–121, 2008.
- [60] W. Sun, S. Zhang, Z. Liu, C. Wang, and Z. Mao, "Studies on the enhanced photocatalytic hydrogen evolution over Pt/PEG-modified TiO₂ photocatalysts," *International Journal of Hydrogen Energy*, vol. 33, no. 4, pp. 1112–1117, 2008.
- [61] H. Abe, T. Kimitani, and M. Naito, "Influence of NH₃/Ar plasma irradiation on physical and photocatalytic properties

- of TiO₂ nanopowder," *Journal of Photochemistry and Photobiology A*, vol. 183, no. 1-2, pp. 171–175, 2006.
- [62] M. Bettinelli, V. Dallacasa, D. Falcomer et al., "Photocatalytic activity of TiO₂ doped with boron and vanadium," *Journal of Hazardous Materials*, vol. 146, no. 3, pp. 529–534, 2007.
- [63] J. R. Xiao, T. Y. Peng, R. Li, Z. H. Peng, and C. H. Yan, "Preparation, phase transformation and photocatalytic activities of cerium-doped mesoporous titania nanoparticles," *Journal of Solid State Chemistry*, vol. 179, no. 4, pp. 1161–1170, 2006.
- [64] E. A. Kozlova and A. V. Vorontsov, "Influence of mesoporous and platinum-modified titanium dioxide preparation methods on photocatalytic activity in liquid and gas phase," *Applied Catalysis B*, vol. 77, no. 1-2, pp. 35–45, 2007.
- [65] C. Wang, Y. H. Ao, P. F. Wang, J. Hou, J. Qian, and S. H. Zhang, "Preparation, characterization, photocatalytic properties of titania hollow sphere doped with cerium," *Journal of Hazardous Materials*, vol. 178, no. 1–3, pp. 517–521, 2010.
- [66] J. J. Xu, Y. H. Ao, M. D. Chen, and D. G. Fu, "Low-temperature preparation of Boron-doped titania by hydrothermal method and its photocatalytic activity," *Journal of Alloys and Compounds*, vol. 484, no. 1-2, pp. 73–79, 2009.
- [67] C. Jin, R. Y. Zheng, Y. Guo, J. L. Xie, Y. X. Zhu, and Y. C. Xie, "Hydrothermal synthesis and characterization of phosphorous-doped TiO₂ with high photocatalytic activity for methylene blue degradation," *Journal of Molecular Catalysis A*, vol. 313, no. 1-2, pp. 44–48, 2009.
- [68] K. J. A. Raj, A. V. Ramaswamy, and B. Viswanathan, "Surface area, pore size, and particle size engineering of titania with seeding technique and phosphate modification," *Journal of Physical Chemistry C*, vol. 113, no. 31, pp. 13750–13757, 2009.
- [69] F. Peng, L. F. Cai, L. Huang, H. Yu, and H. J. Wang, "Preparation of nitrogen-doped titanium dioxide with visible-light photocatalytic activity using a facile hydrothermal method," *Journal of Physics and Chemistry of Solids*, vol. 69, no. 7, pp. 1657–1664, 2008.
- [70] J. Senthilnathan and L. Philip, "Photocatalytic degradation of lindane under UV and visible light using N-doped TiO₂," *Chemical Engineering Journal*, vol. 161, no. 1-2, pp. 83–92, 2010.
- [71] H. Tian, J. Ma, K. Li, and J. Li, "Hydrothermal synthesis of S-doped TiO₂ nanoparticles and their photocatalytic ability for degradation of methyl orange," *Ceramics International*, vol. 35, no. 3, pp. 1289–1292, 2009.
- [72] W. K. Ho, J. C. Yu, and S. C. Lee, "Low-temperature hydrothermal synthesis of S-doped TiO₂ with visible light photocatalytic activity," *Journal of Solid State Chemistry*, vol. 179, no. 4, pp. 1171–1176, 2006.
- [73] X. Chen and S. S. Mao, "Titanium dioxide nanomaterials: synthesis, properties, modifications and applications," *Chemical Reviews*, vol. 107, no. 7, pp. 2891–2959, 2007.
- [74] S. Livraghi, K. Elghniji, A. M. Czoska, M. C. Paganini, E. Giamello, and M. Ksibi, "Nitrogen-doped and nitrogen-fluorine-codoped titanium dioxide. Nature and concentration of the photoactive species and their role in determining the photocatalytic activity under visible light," *Journal of Photochemistry and Photobiology A*, vol. 205, no. 2-3, pp. 93–97, 2009.
- [75] J. G. Yu, W. G. Wang, B. Cheng, and B. L. Su, "Enhancement of photocatalytic activity of Mesoporous TiO₂ powders by hydrothermal surface fluorination treatment," *Journal of Physical Chemistry C*, vol. 113, no. 16, pp. 6743–6750, 2009.
- [76] S. Hu, A. Wang, X. Li, and H. Löwe, "Hydrothermal synthesis of well-dispersed ultrafine N-doped TiO₂ nanoparticles with enhanced photocatalytic activity under visible light," *Journal of Physics and Chemistry of Solids*, vol. 71, no. 3, pp. 156–162, 2010.
- [77] H. Sun, S. Wang, H. M. Ang, M. O. Tadé, and Q. Li, "Halogen element modified titanium dioxide for visible light photocatalysis," *Chemical Engineering Journal*, vol. 162, no. 2, pp. 437–447, 2010.
- [78] K. Mori, K. Maki, S. Kawasaki, S. Yuan, and H. Yamashita, "Hydrothermal synthesis of TiO₂ photocatalysts in the presence of NH₄ F and their application for degradation of organic compounds," *Chemical Engineering Science*, vol. 63, no. 20, pp. 5066–5070, 2008.
- [79] C. L. Yu, J. C. Yu, and M. Chan, "Sonochemical fabrication of fluorinated mesoporous titanium dioxide microspheres," *Journal of Solid State Chemistry*, vol. 182, no. 5, pp. 1061–1069, 2009.
- [80] N. Todorova, T. Giannakopoulou, T. Vaimakis, and C. Trapalis, "Structure tailoring of fluorine-doped TiO₂ nanostructured powders," *Materials Science and Engineering B*, vol. 152, no. 1–3, pp. 50–54, 2008.
- [81] J. Xu, Y. Ao, D. Fu, and C. Yuan, "Synthesis of fluorine-doped titania-coated activated carbon under low temperature with high photocatalytic activity under visible light," *Journal of Physics and Chemistry of Solids*, vol. 69, no. 10, pp. 2366–2370, 2008.
- [82] A. Zaleska, J. W. Sobczak, E. Grabowska, and J. Hupka, "Preparation and photocatalytic activity of boron-modified TiO₂ under UV and visible light," *Applied Catalysis B*, vol. 78, no. 1-2, pp. 92–100, 2008.
- [83] E. Grabowska, A. Zaleska, J. W. Sobczak, M. Gazda, and J. Hupka, "Boron-doped TiO₂: characteristics and photoactivity under visible light," *Procedia Chemistry*, vol. 1, no. 2, pp. 1553–1559, 2009.
- [84] M. Estruga, C. Domingo, X. Domènech, and J. A. Ayllón, "Zirconium-doped and silicon-doped TiO₂ photocatalysts synthesis from ionic-liquid-like precursors," *Journal of Colloid and Interface Science*, vol. 344, no. 2, pp. 327–333, 2010.
- [85] R. Jin, Z. Wu, Y. Liu, B. Jiang, and H. Wang, "Photocatalytic reduction of NO with NH₃ using Si-doped TiO₂ prepared by hydrothermal method," *Journal of Hazardous Materials*, vol. 161, no. 1, pp. 42–48, 2009.
- [86] C. He, B. Tian, and J. Zhang, "Thermally stable SiO₂-doped mesoporous anatase TiO₂ with large surface area and excellent photocatalytic activity," *Journal of Colloid and Interface Science*, vol. 344, no. 2, pp. 382–389, 2010.
- [87] D. Li, H. Haneda, N. K. Labhsetwar, S. Hishita, and N. Ohashi, "Visible-light-driven photocatalysis on fluorine-doped TiO₂ powders by the creation of surface oxygen vacancies," *Chemical Physics Letters*, vol. 401, no. 4–6, pp. 579–584, 2005.
- [88] Q. Zhang, Y. Li, E. A. Ackerman, M. Gajdardziska-Josifovska, and H. Li, "Visible light responsive iodine-doped TiO₂ for photocatalytic reduction of CO₂ to fuels," *Applied Catalysis A*, vol. 400, no. 1-2, pp. 195–202, 2011.
- [89] W.-A. Wang, Q. Shi, Y.-P. Wang, J.-L. Cao, G.-Q. Liu, and P.-Y. Peng, "Preparation and characterization of iodine-doped mesoporous TiO₂ by hydrothermal method," *Applied Surface Science*, vol. 257, no. 8, pp. 3688–3696, 2011.
- [90] Y. Ma, J.-W. Fu, X. Tao, X. Li, and J.-F. Chen, "Low temperature synthesis of iodine-doped TiO₂ nanocrystallites with enhanced visible-induced photocatalytic activity," *Applied Surface Science*, vol. 257, no. 11, pp. 5046–5051, 2011.
- [91] R. Long, Y. Dai, and B. Huang, "Structural and electronic properties of iodine-doped anatase and rutile TiO₂," *Computational Materials Science*, vol. 45, no. 2, pp. 223–228, 2009.

- [92] N. Lu, H. Zhao, J. Li, X. Quan, and S. Chen, "Characterization of boron-doped TiO₂ nanotube arrays prepared by electrochemical method and its visible light activity," *Separation and Purification Technology*, vol. 62, no. 3, pp. 668–673, 2008.
- [93] W. Shi, Q. Chen, Y. Xu, D. Wu, and C.-F. Huo, "Investigation of the silicon concentration effect on Si-doped anatase TiO₂ by first-principles calculation," *Journal of Solid State Chemistry*, vol. 184, no. 8, pp. 1983–1988, 2011.
- [94] C. Wen, Y. J. Zhu, T. Kanbara, H. Z. Zhu, and C. F. Xiao, "Effects of I and F codoped TiO₂ on the photocatalytic degradation of methylene blue," *Desalination*, vol. 249, no. 2, pp. 621–625, 2009.
- [95] R. Niishiro, R. Konta, H. Kato, W. J. Chun, K. Asakura, and A. Kudo, "Photocatalytic O₂ evolution of rhodium and antimony-codoped rutile-type TiO₂ under visible light irradiation," *Journal of Physical Chemistry C*, vol. 111, no. 46, pp. 17420–17426, 2007.
- [96] Y. F. Ma, J. L. Zhang, B. Z. Tian, F. Chen, and L. Z. Wang, "Synthesis and characterization of thermally stable Sm,N co-doped TiO₂ with highly visible light activity," *Journal of Hazardous Materials*, vol. 182, no. 1–3, pp. 386–393, 2010.
- [97] C. R. Estrellan, C. Salim, and H. Hinode, "Photocatalytic decomposition of perfluorooctanoic acid by iron and niobium co-doped titanium dioxide," *Journal of Hazardous Materials*, vol. 179, no. 1–3, pp. 79–83, 2010.
- [98] J. X. Li, J. H. Xu, W.-L. Dai, H. Li, and K. Fan, "One-pot synthesis of twist-like helix tungsten-nitrogen-codoped titania photocatalysts with highly improved visible light activity in the abatement of phenol," *Applied Catalysis B*, vol. 82, no. 3–4, pp. 233–243, 2008.
- [99] R. Khan, S. W. Kim, T.-J. Kim, and C.-M. Nam, "Comparative study of the photocatalytic performance of boron-iron Co-doped and boron-doped TiO₂ nanoparticles," *Materials Chemistry and Physics*, vol. 112, no. 1, pp. 167–172, 2008.
- [100] J. G. Yu, M. H. Zhou, B. Cheng, and X. J. Zhao, "Preparation, characterization and photocatalytic activity of in situ N,S-codoped TiO₂ powders," *Journal of Molecular Catalysis A*, vol. 246, no. 1–2, pp. 176–184, 2006.
- [101] C. Yu, D. Cai, K. Yang, J. C. Yu, Y. Zhou, and C. Fan, "Sol-gel derived S,I-codoped mesoporous TiO₂ photocatalyst with high visible-light photocatalytic activity," *Journal of Physics and Chemistry of Solids*, vol. 71, no. 9, pp. 1337–1343, 2010.
- [102] F. Wei, L. Ni, and P. Cui, "Preparation and characterization of N-S-codoped TiO₂ photocatalyst and its photocatalytic activity," *Journal of Hazardous Materials*, vol. 156, no. 1–3, pp. 135–140, 2008.
- [103] M. Hamadani, A. Reisi-Vanani, and A. Majedi, "Synthesis, characterization and effect of calcination temperature on phase transformation and photocatalytic activity of Cu,S-codoped TiO₂ nanoparticles," *Applied Surface Science*, vol. 256, no. 6, pp. 1837–1844, 2010.
- [104] Y. Xie, X. J. Zhao, Y. Z. Li, Q. N. Zhao, X. D. Zhou, and Q. Yuan, "CTAB-assisted synthesis of mesoporous F-N-codoped TiO₂ powders with high visible-light-driven catalytic activity and adsorption capacity," *Journal of Solid State Chemistry*, vol. 181, no. 8, pp. 1936–1942, 2008.
- [105] L. Y. Li, Z. Y. Xu, F. L. Liu et al., "Photocatalytic nitrate reduction over Pt-Cu/TiO₂ catalysts with benzene as hole scavenger," *Journal of Photochemistry and Photobiology A*, vol. 212, no. 2–3, pp. 113–121, 2010.
- [106] Y. Wu, J. Zhang, L. Xiao, and F. Chen, "Properties of carbon and iron modified TiO₂ photocatalyst synthesized at low temperature and photodegradation of acid orange 7 under visible light," *Applied Surface Science*, vol. 256, no. 13, pp. 4260–4268, 2010.
- [107] T. Sreethawong, S. Laehsatee, and S. Chavadej, "Use of Pt/N-doped mesoporous-assembled nanocrystalline TiO₂ for photocatalytic H₂ production under visible light irradiation," *Catalysis Communications*, vol. 10, no. 5, pp. 538–543, 2009.
- [108] S. K. Biswas, A. Pathak, N. K. Pramanik, D. Dhak, and P. Pramanik, "Codoped Cr and W rutile nanosized powders obtained by pyrolysis of triethanolamine complexes," *Ceramics International*, vol. 34, no. 8, pp. 1875–1883, 2008.
- [109] G. Colón, M. Maicu, M. C. Hidalgo, J. A. Navío, A. Kubacka, and M. Fernández-García, "Gas phase photocatalytic oxidation of toluene using highly active Pt doped TiO₂," *Journal of Molecular Catalysis A*, vol. 320, no. 1–2, pp. 14–18, 2010.
- [110] N. A. Jamalluddin and A. Z. Abdullah, "Reactive dye degradation by combined Fe(III)/TiO₂ catalyst and ultrasonic irradiation: effect of Fe(III) loading and calcination temperature," *Ultrasonics Sonochemistry*, vol. 18, no. 2, pp. 669–678, 2011.
- [111] C. H. Chiou and R. S. Juang, "Photocatalytic degradation of phenol in aqueous solutions by Pr-doped TiO₂ nanoparticles," *Journal of Hazardous Materials*, vol. 149, no. 1, pp. 1–7, 2007.
- [112] C. Suwanchawalit and S. Wongnawa, "Influence of calcination on the microstructures and photocatalytic activity of potassium oxalate-doped TiO₂ powders," *Applied Catalysis A*, vol. 338, no. 1–2, pp. 87–99, 2008.
- [113] T. J. Kemp and R. A. McIntyre, "Transition metal-doped titanium(IV) dioxide: characterisation and influence on photodegradation of poly(vinyl chloride)," *Polymer Degradation and Stability*, vol. 91, no. 1, pp. 165–194, 2006.
- [114] L. Andronic, A. Enesca, C. Vladuta, and A. Duta, "Photocatalytic activity of cadmium doped TiO₂ films for photocatalytic degradation of dyes," *Chemical Engineering Journal*, vol. 152, no. 1, pp. 64–71, 2009.
- [115] C. Sahoo, A. K. Gupta, and A. Pal, "Photocatalytic degradation of Crystal Violet (C.I. Basic Violet 3) on silver ion doped TiO₂," *Dyes and Pigments*, vol. 66, no. 3, pp. 189–196, 2005.
- [116] Q. Xiao, J. Zhang, C. Xiao, Z. Si, and X. Tan, "Solar photocatalytic degradation of methylene blue in carbon-doped TiO₂ nanoparticles suspension," *Solar Energy*, vol. 82, no. 8, pp. 706–713, 2008.
- [117] S. Yang, W. Zhu, J. Wang, and Z. Chen, "Catalytic wet air oxidation of phenol over CeO₂-TiO₂ catalyst in the batch reactor and the packed-bed reactor," *Journal of Hazardous Materials*, vol. 153, no. 3, pp. 1248–1253, 2008.
- [118] L. G. Devi and K. E. Rajashekhar, "A kinetic model based on non-linear regression analysis is proposed for the degradation of phenol under UV/solar light using nitrogen doped TiO₂," *Journal of Molecular Catalysis A*, vol. 334, no. 1–2, pp. 65–76, 2011.
- [119] Y. Lv, L. Yu, H. Huang, H. Liu, and Y. Feng, "Preparation, characterization of P-doped TiO₂ nanoparticles and their excellent photocatalytic properties under the solar light irradiation," *Journal of Alloys and Compounds*, vol. 488, no. 1, pp. 314–319, 2009.
- [120] J. Gong, C. Yang, W. Pu, and J. Zhang, "Liquid phase deposition of tungsten doped TiO₂ films for visible light photoelectrocatalytic degradation of dodecyl-benzenesulfonate," *Chemical Engineering Journal*, vol. 167, no. 1, pp. 190–197, 2011.
- [121] N. Venkatachalam, M. Palanichamy, B. Arabindoo, and V. Murugesan, "Enhanced photocatalytic degradation of

- 4-chlorophenol by Zr^{4+} doped nano TiO_2 ,” *Journal of Molecular Catalysis A*, vol. 266, no. 1-2, pp. 158–165, 2007.
- [122] J. Sun, X. Wang, J. Sun, R. Sun, S. Sun, and L. Qiao, “Photocatalytic degradation and kinetics of Orange G using nano-sized $Sn(IV)/TiO_2/AC$ photocatalyst,” *Journal of Molecular Catalysis A*, vol. 260, no. 1-2, pp. 241–246, 2006.
- [123] J. Wang, W. Sun, Z. Zhang et al., “Preparation of Fe-doped mixed crystal TiO_2 catalyst and investigation of its sonocatalytic activity during degradation of azo fuchsine under ultrasonic irradiation,” *Journal of Colloid and Interface Science*, vol. 320, no. 1, pp. 202–209, 2008.
- [124] N. Sobana, K. Selvam, and M. Swaminathan, “Optimization of photocatalytic degradation conditions of Direct Red 23 using nano-Ag doped TiO_2 ,” *Separation and Purification Technology*, vol. 62, no. 3, pp. 648–653, 2008.



Hindawi

Submit your manuscripts at
<http://www.hindawi.com>

